Translational Oncology 14 (2021) 100918

Contents lists available at ScienceDirect

Translational Oncology

journal homepage: www.elsevier.com/locate/tranon

TIM3 expression on tumor cells predicts response to anti-PD-1 therapy for renal cancer

Renpei Kato[a,*], Noriaki Jinnouchi[a], Takashi Tuyukubo[a,b], Daiki Ikarashi[a], Tomohiko Matsuura[a], Shigekatsu Maekawa[a], Yoichiro Kato[a], Mitsugu Kanehira[a], Ryo Takata[a], Kazuyuki Ishida[b,c], Wataru Obara[a]

[a] Department of Urology, Iwate Medical University, Morioka-city, Japan
[b] Department of Molecular Diagnostic Pathology, Iwate Medical University, Shiwa, Iwate, Japan
[c] Department of Molecular Diagnostic Pathology, Dokkyo Medical University, Shimotsuga, Tochigi, Japan

ARTICLE INFO

Keywords:
TIM3
Renal cancer
Anti-PD-1 therapy

ABSTRACT

This study aimed to identify novel prognostic biomarker for advanced renal cell carcinoma (RCC) patients treated with anti-PD-1 therapy, using quantitative multi-immunofluorescence (IF) analysis of tumor immunity. Twenty-five consecutive patients who had metastatic or unresectable RCC treated with anti-PD-1 therapy were studied. The patients were divided into a responder group ($n=12$) and a non-responder group ($n=13$). Quantitative multi-IF staining was performed on biopsy or surgical kidney samples using a panel of antibodies. Sections were scanned using a Mantra microscope, and the images were analyzed with inForm™ software. Responders had significantly higher rate of TIM3-positive tumor (100% versus 53.9%, $p < 0.01$) than non-responders. Multi-IF analysis showed that TIM3 expression on tumor cells was most strongly related to response to anti-PD-1 therapy, while some of the known immune-related prognostic factors in RCC (CD45RO, FOXP3, VEGF, PD-L1, PD-L2, CD163) had no significant association. Patients with TIM3-positive tumor showed significantly longer overall survival (not reached median time versus 6.0 months, $p < 0.01$) and progression-free survival (18.9 versus 1.1 months, $p < 0.01$) than those with TIM3-negative tumor. Immunohistochemistry study using samples obtained after anti-PD-1 therapy showed infiltration of CD163 macrophages and release of HMGB1, a ligand of TIM3, in necrotic tumor area. In conclusion, our study found clinical correlation between TIM3 expression on tumor cells and response to anti-PD-1 therapy. Further studies are warranted to verify whether TIM3 expression on tumor cells before systemic therapy predicts the efficacy of anti-PD-1 therapy for RCC in the clinical setting.

Introduction

Renal cell carcinoma (RCC) represents 2–4% of all malignancies. In the US, the figures estimated for 2020 are 73,750 new RCC cases and 14,830 deaths [1]. Approximately 20% of RCC cases are metastatic disease, and 5-year relative survival rate of metastatic cases is only 10%.

Recent phase III studies provided evidence for the accelerated approval of immuno-oncology (IO) therapy targeting the PD-1/PD-L1 axis for metastatic RCC [2–5]. Availability of a biomarker that predicts responders and non-responders to anti-PD-1 therapy would minimize unnecessary exposure of patients to potentially immune-related toxicities and reduce the financial burden on health systems because these treatments are expensive. However, useful biomarker has not yet been established [6–8].

Recent study reveals a dynamic relationship between host immunity and tumor in the process of carcinogenesis. The tumor acquires the ability to evade recognition by the host immune systems [9]. Although accumulating evidence has revealed that tumor-infiltrating lymphocytes (TILs), tumor-associated macrophages (TAMs), VEGF, PD-L1, PD-L2 and TIM3 have diverse tumorigenic activities in RCC, some contradictory findings were also reported. Regarding TILs, FOXP3-positive CD4 T cells [10], FOXP3-negative CD4 T cells [11], CD45RO-expressing

Abbreviations: RCC, renal cell carcinoma; IO, immuno-oncology; IF, immunofluorescence; Nivo, Nivolumab; Nivo+Ipi, Nivolumab plus Ipilimumab combination; PFS, progression-free survival; OS, overall survival; FFPE, formalin-fixed and paraffin-embedded; TILs, tumor-infiltrating lymphocytes; TAMs, tumor-associated macrophages; IHC, immunohistochemistry; KPS, Karnofsky performance status; IMDC, the International Metastatic RCC Database Consortium; BOR, best overall response; CR, complete response; PR, partial response; SD, stable disease; PD, progressive disease; pT, pathological tumor; HMGB1, the nuclear DNA-binding protein high mobility group box 1 protein.

* Corresponding author.
E-mail address: rekato@iwate-med.ac.jp (R. Kato).

https://doi.org/10.1016/j.tranon.2020.100918
Received 23 August 2020; Received in revised form 27 September 2020; Accepted 12 October 2020

T cells [12], and TIM3-positive CD8 T-cells [13] were associated with poor prognosis of RCC. For TAMs, CD163-positive macrophages were shown to be an indicator of poor clinical outcome in RCC [14]. VEGF is not only a pro-angiogenic molecule but also a regulator of tumor immunity [15]. VEGF expression was an indicator of adverse prognosis in RCC [16]. PD-L1 expression on tumor cells was associated with shorter survival in RCC patients treated with sunitinib or pazopanib [17], while PD-L2 was a predictor of longer progression-free survival (PFS) in cancer cohorts including RCC patients [18]. TIM3 is frequently expressed on RCC tumor tissue, and higher TIM3 expression level was a predictor of shorter PFS in patients receiving systemic therapy [19]. However, the subjects of the above studies were treated with cytokines or targeted therapy. Therefore, the clinical relevance of these immune-related factors remains uncertain in the era of IO therapy.

Multi-immunofluorescence (Multi-IF) staining that allows identification of several targets in the same tissue section is an invaluable tool for tumor immune-profiling and development of novel predictive biomarkers for cancer immunotherapy [20]. The use of software to compute the pure spectrum of a fluorophore from mixed emission signals, combined with automated image analysis avoids the usual risk of overlapping signals from various fluorophores and inter-operator variability of manual counting. In this study, we aimed to identify novel prognostic biomarker for advanced RCC patients treated with anti-PD-1 therapy using quantitative multi-IF analysis to examine host and tumor immunity.

Materials and methods

Patients

This study was a retrospective study by reviewing medical records at our institution during the period of September 2016 to May 2019. Twenty-five consecutive patients who had a confirmed diagnosis of metastatic or unresectable RCC and received anti-PD-1 therapy were enrolled in the study. Fifteen patients were treated with nivolumab monotherapy (Nivo monotherapy) following targeted therapy, and 10 patients with nivolumab plus ipilimumab combination therapy (Nivo+Ipi therapy) as first-line therapy. All patients underwent diagnostic CT-guided biopsy or therapeutic nephrectomy before systemic therapy. Treatments for the subjects were planned according to standard of care in accordance with relevant treatment guidelines. From the medical records, clinical data including medical history, treatment duration, reason for discontinuation, types of targeted therapy prior to Nivo monotherapy, PFS and overall survival (OS) were collected. Tumor assessments were conducted at baseline, week 12 and every 12 weeks thereafter. According to response to anti-PD-1 therapy, we divided our patients into a responder group and a non-responder group [21]. Responder was defined as a patient who achieved complete or partial response (excluding mixed responses) to anti-PD-1 therapy. Non-responder was defined as a patient who had progressive disease or stable disease control. These response patterns were based on RECIST ver.1.1.

This study was conducted in accordance with the ethical principles of the Declaration of Helsinki. The institutional review board of our institution approved the present study (approval number: H29-18). Informed consent was waived by the institutional review board.

Multi-IF staining of pretreatment samples

Formalin-fixed and paraffin-embedded (FFPE) kidney tissue samples were obtained from patients before starting systemic therapy. The biopsy or surgical tissue samples were fixed in 10% neutral buffered formalin and embedded in paraffin per routine methods. The quality of each sample was checked by two pathologists who examined a hematoxylin-eosin (HE)-stained section. Multi-IF staining was performed as described previously [13,20]. Anti-CD4, -CD8, -CD45RO, -FOXP3 and -TIM3 antibodies were used for detecting tumor-infiltrating lymphocytes (TILs) [10–13,22]. Anti-CD68 and CD163 antibodies were used for detecting tumor-associated macrophages (TAMs) [14]. Anti-VEGF, PD-L1, PD-L2, TIM3 and pan-cytokeratin AE1/AE3 antibodies were used to detect the expression of these molecules on tumor tissues [16–19,23]. These antibodies are described in Supplementary Table 1. We determined the best antibody sequence in multiplex staining for each panel combination: panel 1 (pan-cytokeratin AE1/AE3, CD4, CD8, CD45RO, FOXP3, TIM3 and DAPI) and panel 2 (VEGF, PD-L1, PD-L2, CD68, CD163 and DAPI). Sections without addition of primary antibody were used as negative controls in all specimens. To detect six protein biomarkers on the same tissue section, Opal™ 7 Immunology Discovery Kit (ParkinElmer, Life Science, Waltham, MA, USA) was used as the fluorophore (Supplementary Table 1). In each case, we checked that secondary antibodies did not cross-react with unrelated primary antibodies used in the combination. Nuclei were counterstained using a DAPI mounting medium.

Quantitative fluorescent staining

Slides of stained specimens were read under a Mantra microscope (ParkinElmer, Life Science, Waltham, MA, USA) following the previously published protocol [24]. For each specimen, after low magnification scanning at × 10, individual fields were sampled randomly [five fields for biopsy specimen, 10 fields (5 fields from central area and 5 fields from peripheral area of the tumor) for surgical specimen] in the intra-tumoral compartment for scanning at higher magnification (× 20) in order to capture various elements of tumor heterogeneity. Histologic assessment of each area analyzed was performed to ensure that tumor tissue (based on expression of pan-cytokeratin AE1/AE3) was included in the selected intra-tumoral region.

The data acquired with the multispectral camera were processed by the inForm™ software (ParkinElmer, Life Science, Waltham, MA, USA), which allows automated cell segmentation and phenotyping. Cell recognition was based on DAPI staining. Then, a phenotyping step, which was based on teaching the software to recognize positive and negative cells, was performed to define an algorithm program of analysis.

Investigation of types of TILs was performed as follows. Cells co-stained for CD4 and CD45RO and/or FOXP3 ($CD4^+CD45RO^+FOXP3^+$ and $CD4^+CD45RO^+FOXP3^-$), and cells mono-stained for CD8 ($CD8^+CD45RO^-TIM3^-$) or co-stained for CD8 and CD45RO ($CD8^+CD45RO^+$ $TIM3^-$) or TIM3 ($CD8^+CD45RO^-TIM3^+$) were identified manually based on fluorescence intensity and subcellular localization of staining, and counted until automatized recognition by the inForm™ 2.4 software was concordant with visual count (Fig. 1A). The mean number of positive-stained cells in at least 5 fields of biopsy specimen and 10 fields of surgical specimen was calculated. For the phenotyping step, an independent operator confirmed the visual inspection. Each phenotyping image was checked after software analysis.

Investigation of TAMs was performed as follows. Quantitative analyses of CD63 and CD163 staining on macrophages were also performed with the inForm™ 2.4 software after acquiring images by the Mantra microscope (Fig. 1B).

For quantification of the expression of PD-L1, PD-L2, VEGF, and TIM3 on the tumor, intensity of staining was analyzed by the inForm™ 2.3 software and scored on a scale of 0 to +3, and H-score was calculated as the sum of intensity multiplied by percentage of staining area (Fig. 1C). Positive staining on tumor was defined as subcellular localization of staining and immunohistochemistry (IHC) score > 15.

Immunostaining and quantification analyses for expression of TIM3 and TIM3-related molecules in post-anti-PD-1 therapy samples

Immunostaining was performed using post-treatment samples obtained from 5 patients (3 patients on Nivo monotherapy, 2 patients on Nivo+Ipi therapy). Tumor response was checked by examining the

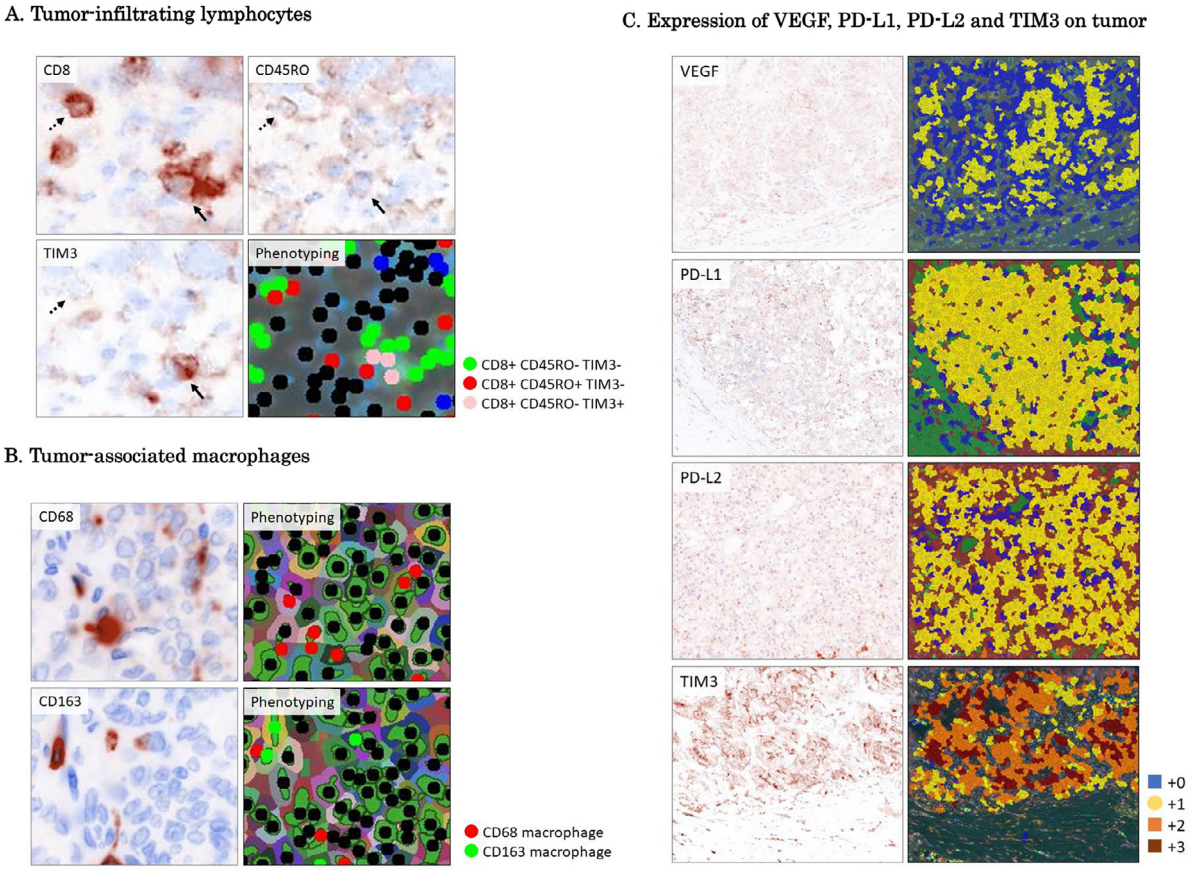

Fig. 1. Quantitative fluorescent staining.
A. Tumor-infiltrating lymphocytes: Fluorescent staining shows expansion of CD8, CD45RO and TIM3. Cells mono-stained for CD8 ($CD8^+CD45RO^-TIM3^-$) or co-stained for CD8 and CD45RO ($CD8^+CD45RO^+$ $TIM3^-$) or TIM3 ($CD8^+$ $CD45RO^-TIM3^+$) were recognized by the inForm™ 2.4 software. CD8+CD45RO+ TIM3- cells are indicated by the arrow. CD8+ CD45RO-TIM3+ are indicated by the dotted arrow.
B. Tumor-associated macrophages: Fluorescent staining shows expansion of CD68 and CD163. Cells stained for CD68 or CD163 were recognized by the inForm™ 2.4 software.
C. Expression of VEGF, PD-L1, PD-L2 and TIM3 on tumor: For quantification of the expression of PD-L1, PD-L2, VEGF, and TIM3 on tumor, intensity of staining was analyzed by the inForm™ 2.3 software and scored on a scale of 0 to +3, and H-score .

intra-tumoral compartment in an HE-stained section by two pathologists. Necrotic area, which is an indication of response to anti-PD-1 therapy, and viable tumor area, which is an indication of refractoriness to anti-PD-1 therapy, were selected from the sample, and immunostaining was performed for the following molecules. High mobility group protein B1 (HMGB1) antibody was used for evaluation of TIM3-interacting partner related to tumor immunity [25] and CD163 antibody was used for detecting TAMs [14]. The primary antibodies and secondary antibodies used in immunostaining are described in Supplementary Table 2. Images were acquired from selected areas showing necrosis and areas showing viable tumor cells.

Bioinformatic analysis for TIM3 gene alteration

The status of TIM3 gene in RCC was investigated on cBioPortal OncoPrint (http://www.cBioPortal.org/index.do) using the data for The Cancer Genome Atlas (TCGA) Pan-Cancer Atlas (PanCanAtlas) cohort [26,27]

Statistical analysis

Fisher's exact test and *t*-test were used to compare patient characteristics. Correlation was analyzed using the Spearman rank correlation test. Logistic regression analysis was used for multivariate statistical analysis. PFS and OS were estimated by the Kaplan-Meier method. Univariate analyses were performed by the log-rank test. *P* value less than 0.05 was considered to indicate statistical significance in all tests. Statistical analyses were performed using JMP14 (SAS Institute, Cary, NC, USA).

Results

Patient characteristics

Table 1 shows patient characteristics. The subjects comprised 20 men and 5 women with mean age of 65.9 ± 2.0 years. Sixteen patients had Karnofsky performance status (KPS) score of 80 to 100% (mean 82.0 ± 3.1%) at the start of anti-PD-1 therapy. According to the International Metastatic RCC Database Consortium (IMDC) risk criteria, 11 patients (44%) were classified as intermediate risk and 11 patients (44%) as poor risk. Nine patients (36%) had renal tumors with inferior vena caval extension (clinical T3b or T3c) or involving adjacent organ (clinical T4). The most common sites of metastases were lung (21 patients, 84%), bone (10 patients, 40%) and lymph nodes (9 patients, 36%). Fifteen patients were treated with Nivo monotherapy as second-line therapy after targeted therapy and 10 patients were treated with Nivo+Ipi therapy as first-line therapy. Tissue samples were collected by surgery in 10 patients and by CT-guided biopsy in 15 patients. The median follow-up period was 16.4 months (95% confidence interval [CI] 11.8–20.3).

Table 1
Patient characteristics of responder and non-responder groups.

Characteristics	Responders $n=12$	Non-responders $n=13$	p value
Age, year	67.1 ± 3.0	64.8 ± 2.7	0.57
Sex (men), *n* (%)	10 (83.3)	10 (76.9)	1.00
KPS≥80%, *n* (%)	2 (16.7)	7 (53.9)	0.10
MSKCC favorable/intermediate/poor risk, n	3/4/5	0/6/7	0.16
IMDC favorable/intermediate/poor risk, n	3/4/5	0/7/6	0.14
Histological clear cell subtype, *n* (%)	11 (91.7)	9 (69.2)	0.32
T stage cT3b/3c/4, *n* (%)	5 (41.7)	4 (30.8)	0.69
Sites of metastases, *n* (%)			
Lung	12 (100)	9 (69.2)	0.10
Liver	4 (33.3)	2(15.4)	0.38
Bone	4 (33.3)	6 (46.2)	0.69
Lymph nodes	3 (25.0)	6 (46.2)	0.41
Prior nephrectomy, *n* (%)	6 (50.0)	5 (38.5)	0.70
Immuno-checkpoint inhibitor, *n* (%)			
Nivo monotherapy	8 (66.7)	7 (53.9)	0.69
Nivo+Ipi therapy	4 (33.3)	6 (46.1)	
TTF in Nivo mono therapy group, months (mean±SD)	16.1 ± 8.6	6.5 ± 3.8	0.33
BOR to IO therapy: CR/PR/SD/PD, *n*	1/11/0/0	0/0/8/5	<0.01
Reason of discontinuation of TT in Nivo mono therapy group; AE/PD/Ope, *n*	2/6/0	1/5/1	0.51
PFS, months (mean±SD)	12.3 ± 2.5	9.0 ± 2.2	0.34
OS, months (mean±SD)	20.8 ± 3.1	11.6 ± 2.1	0.02
Procedure to collect tissue sample, *n* (%)	5 (41.7)	5 (38.5)	0.70
Surgery	7 (58.3)	8 (61.5)	
CT-guided biopsy			

KPS; Karnofsky performance status, MSKCC; Memorial Sloan-Kettering Cancer Center.
IMDC; International Metastatic RCC Database Consortium.
Nivo; nivolumab, Ipi; ipilimumab, TTF; time to treatment failure.
TT; targeted therapy, PFS; progression-free survival, OS; overall survival.
BOR; best overall response.

To evaluate biomarker for predicting response to anti-PD-1 therapy, we performed an analysis by dividing the patients into a responder group ($n=12$) and non-responder group ($n=13$). Patient background did not differ significantly between the two groups. The proportion of patients treated with Nivo+Ipi therapy was similar between the responder and the non-responder groups (33.3% versus 46.1%, $p=0.69$). According to best overall response (BOR) in all patients, 1 case had complete response (CR) case, 11 cases had partial response (PR), 8 cases had stable disease (SD), and 5 cases had progressive disease (PD). In the non-responder group, 5 of 7 cases (71%) treated with Nivo monotherapy had PD, and all 5 cases treated with Nivo+Ipi therapy had SD. The PFS tended to be longer in the responder group than in the non-responder group (12.3 ± 2.5 months versus 9.0 ± 2.2, $p=0.34$). The OS was significantly longer in the responder group than in the non-responder group (20.8 ± 3.1 months versus 11.6 ± 2.1, $p=0.02$).

Comparison of phenotypes of TILs and TAMs between responders and non-responders

We performed a multi-IF analysis to examine phenotypes of TILs and TAMs to identify marker that predicts efficacy before initiation of anti-PD-1 therapy. Results of quantitative analyses for multi-IF staining are summarized in Table 2. First, we analyzed and compared of phenotypes of CD4 T cells and CD8 T cells in tumor between the two groups. The number of $CD4^+CD45RO^+FOXP3^-$ *T* cells was significantly larger in the responder group than in the non-responder group (cell density: 7.9 ± 1.8 versus 2.6 ± 0.6, $p=0.02$). The number of $CD4^+CD45RO^+FOXP3^+$ *T* cells was similar between the two groups. The numbers of $CD8^+CD45RO^-TIM3^-$ *T* cells, $CD8^+CD45RO^+TIM3^-$ *T* cells and $CD8^+$ $CD45RO^-TIM3^+$ *T* cells were also similar between the two groups.

Next, we analyzed infiltration of TAMs in tumor. The number of CD68 macrophages and CD163 macrophages in tumor were similar between the responder group and the non-responder group.

Pretreatment expression of VEGF, PD-L1, PD-L2 and TIM3 on tumor

Expressions of VEGF, PD-L1, PD-L2 and TIM3 on tumor cells in the responder group and the non-responder group were analyzed (Table 2). There were no significant differences between the two groups in the proportions of cases with VEGF-positive tumor, PD-L1-positive tumor and PD-L2-positive tumor. Immunostaining of tumor tissues demonstrated TIM3 expression on both immune cells and tumor cells. We detected TIM3 expression on tumor cells in all the responders. A significant difference in the proportion of cases with TIM3-positive tumor was observed between the responder and non-responder groups (100% versus 53.9%, $p < 0.01$). Expression of pan-cytokeratin AE1/AE3 was similar between the responder group and the non-responder group.

Table 2
Comparison of quantitative multi-immunofluorescence analyses between responders and non-responders.

Quantitative analyses of multi-IF	Responders $n=12$	Non-responders $n=13$	Univariate analysis p value	Multivariate analysis p value
CD4+ CD45RO+ FOXP3-, CD (mean±SD)	7.9 ± 1.8	2.6 ± 0.6	0.02	0.10
CD4+ CD45RO+ FOXP3+, CD (mean±SD)	2.3 ± 1.9	0.7 ± 0.5	0.42	
CD8+ CD45RO- TIM3-, CD (mean±SD)	53.4 ± 18.3	50.3 ± 25.4	0.92	
CD8+ CD45RO+, CD (mean±SD)	38.0 ± 17.9	33.8 ± 12.9	0.85	
CD8+ TIM3+, CD (mean±SD)	15.6 ± 9.9	1.3 ± 0.5	0.18	
CD68+ macrophage in tumor, CD (mean ± SD)	93.5 ± 30.9	88.9 ± 21.2	0.90	
CD163+ macrophage in tumor, CD (mean ± SD)	141.1 ± 19.4	149.3 ± 27.2	0.81	
VEGF positive on tumor, *n* (%)	9 (75.0)	12 (93.1)	0.32	
PD-L1 positive on tumor, *n* (%)	9 (75.0)	8 (61.5)	0.67	
PD-L2 positive on tumor, *n* (%)	10 (83.3)	12 (92.3)	1.00	
Tim3 positive on tumor, *n* (%)	12 (100)	7 (53.9)	0.01	0.01
Pan-CK AE1 AE3 on tumor, H-score	138.9 ± 12.3	151.3 ± 15.0	0.53	

CD; cell density, CK; cytokeratin.

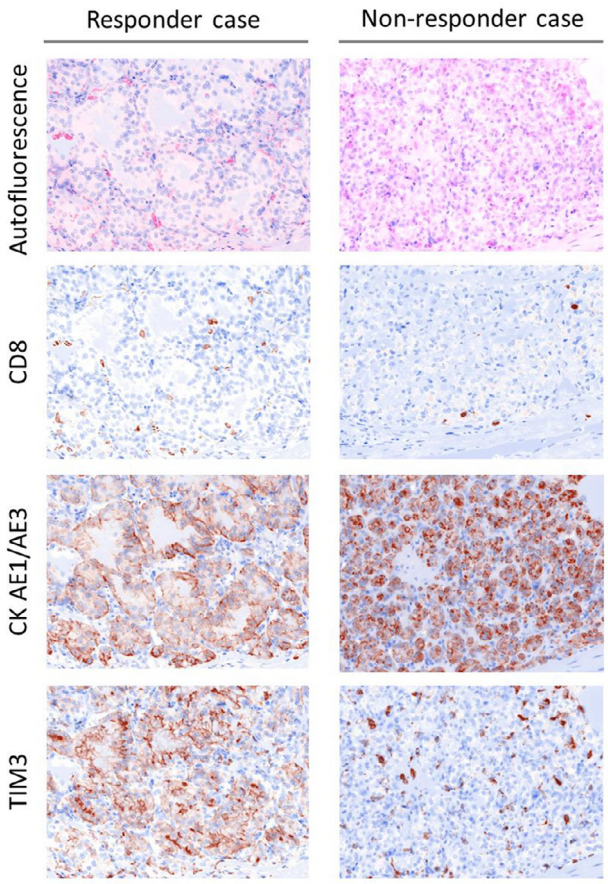

Fig. 2. Multi-immunofluorescence (IF) staining of a responder case and a non-responder case.
Multi-IF demonstrates different TIM3 expression patterns in tumor between the responder case and the non-responder case (magnification: × 20). Responder case (left): TIM3 expression is seen mainly on tumor cells and does not co-express with CD8. Non-responder case (right): TIM3 expression is found mainly in the stroma of tumor. TIM3 expression on tumor cells is considerably low.

Clinical significance of TIM3 expression on tumor cells

An exploratory analysis was performed to evaluate the prognostic relevance of the results of quantitative multi-IF analysis. Multivariate analysis identified TIM3 expression on tumor cell as the only significant independent variable associated with the response to anti-PD-1 therapy (Table 2). Immunostaining of tissues from patients with good response to Nivo monotherapy revealed TIM3 expression mainly on tumor cells with no co-expression with CD8 (Fig. 2, responder case). Immunostaining of tissues from patients with rapidly progressive disease during Nivo monotherapy showed considerably low expression of TIM3 on tumor cells (Fig. 2, non-responder case).

The correlation between TIM3 expression and clinicopathologic factors was then analyzed. Patients with TIM3-positive tumor cells had significantly longer OS and PFS than those with TIM3-negative tumor cells (Fig. 3). In the present study, 6 patients with TIM-3 positive tumor cells were classified into the non-responder group. In a subgroup analysis of the non-responder group, patients with TIM3-positive tumor cells tender to have significantly lower rate of PD (14.3% versus 66.7%, $p = 0.01$), a tendency of longer PFS (12.4 months versus 5.1 months, $p = 0.10$) and apparently longer OS (14.0 months versus 8.8 months, $p = 0.27$) than those with TIM3-negative tumor cells. Patients with TIM3-positive tumor and those with TIM3-negative tumor did not differ in the frequencies of exhibiting pathological characteristics indicating aggressive behavior of RCC [higher pathological tumor stage (pT stage), higher nuclear grade, presence of sarcomatoid differentiation, presence of necrosis, and presence of venous infiltration] (Supplementary Table 3).

Multi-IF analysis of tumors before systemic therapy showed no significant relation between TIM3 expression on tumor and the presence of CD68 or CD163 macrophages (TIM3 versus CD68: $r = -0.19$, $p = 0.38$, TIM3 versus CD163: $r = -0.14$, $p = 0.50$).

To examine the possible mechanism for the difference in TIM3 expression in RCC, we searched for the status of the TIM3 gene in RCC on cBioPortal OncoPrint. According to the results for the TCGA PanCanAtlas cohort ($n = 10{,}967$), 31 of 511 (6%) RCC cases exhibited TIM3 gene amplification. The frequency of alteration of *TIM3* was higher in RCC than in other types of cancer (Supplementary Fig. 1).

Immunostaining of HMGB1 and macrophage infiltration in post-anti-PD-1 therapy sample

TIM3 has been reported to have multiple ligands including galectin 9, phosphatidylserine, CEACAM1 and HMGB1. Among these ligands, HMGB1 is a necrosis-related ligand [28]. The nuclear DNA-binding protein HMGB1 binds to TIM3 and induces phagocytosis by recruiting macrophages and dendritic cells [29]. Previously, our group reported a case of CR treated with Nivo monotherapy [30]. This case exhibited necrotic cell death and infiltration of macrophages in tumor tissue. Therefore, we performed IHC to analyze expression of HMGB1 and infiltration of CD163-positive macrophages in tumor after initiating anti-PD-1 therapy. Five cases were studied. Two cases underwent nephrectomy subsequent to Nivo therapy, two cases underwent nephrectomy subsequent to Nivo+Ipi therapy, and one case (case 3) was autopsied after Nivo monotherapy. The results of IHC are summarized in Table 3 and representative micrographs are shown in Supplementary Fig. 2. HE staining of samples obtained after initiation of anti-PD-1 therapy showed necrotic tumor area in case 1, case 2, case 4 and case 5. TIM3 expression was detected on tumor cells in 4 cases, except in case 3. Low and intranuclear expression of HMGB1 was found in the viable area in cases 2, 3, 4 and 5, and extranuclear expression of HMGB1 was detected in the necrotic area in cases 1, 2, 4 and 5. Accumulation of CD163 macrophages was found only in the necrotic area in cases 1, 2, 4 and 5.

Discussion

We show that TIM3 expression on tumor cells is a potential predictor of efficacy of anti-PD-1 therapy. This is a clinically important predictor that may minimize unnecessary exposure of patients to potentially immune-related toxicities and reduce the financial burden on the health systems because these treatments are expensive with limited efficacy. Multi-IF analysis that allows visualization of several targets in the same tissue section is an invaluable tool for tumor immune-profiling and for the development of novel predictive biomarkers for cancer immunotherapy [20]. In this study, we demonstrated the usefulness of the multi-IF technique to identify novel prognostic biomarker for advanced RCC patients treated with anti-PD-1 therapy.

The strongest prognostic factor of anti-PD-1 therapy identified in this study is the expression of TIM3 on tumor cells. Some of the known immune-related prognostic factors in RCC (CD45RO, FOXP3, VEGF, PD-1, PD-L2, CD163) were not significantly associated with efficacy of anti-PD-1 therapy. $CD4^+CD45RO^+FOXP3$- T cells, despite showing a modest association with efficacy in univariate analysis, was not a significant independent predictor of efficacy in multivariate analysis. Patients showing TIM3-positive tumor cells showed significantly longer OS and PFS than those with TIM3-negative tumor cells. In the non-responder group, TIM3 expression on tumors tended to be associated with lower rate of PD and longer PFS and longer OS. There was no significant relation between pathological characteristics indicating aggressive behavior of RCC and TIM3 expression on tumor cells. Moreover, the proportion of cases with PD-L1 expression on tumor was higher in this study than previous report. Expression of molecules associated with immune evasion

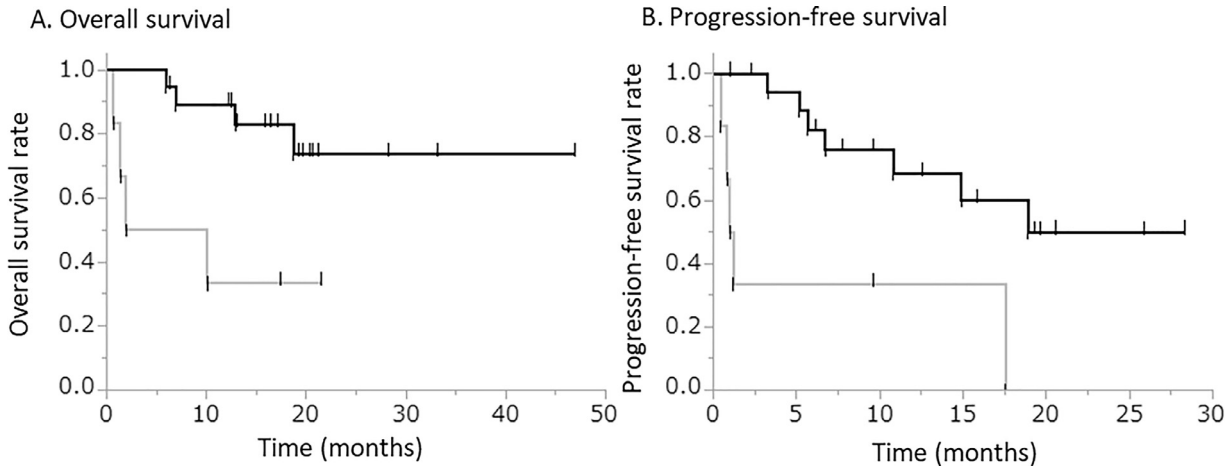

Fig. 3. Clinical significance of TIM3 expression on tumor cells.
Kaplan–Meier curves for the group with TIM3-positive tumor cells (black line) and the group with TIM3-negative tumor cells (gray line) were plotted for overall survival (OS) and progression-free survival (PFS).
A. OS [median (95% confidence interval)] in patients with TIM3-positive tumor cells is significantly longer than in those with TIM3-negative tumor cells [not reached median time (18.7 – not reached) versus 6.0 months (0.7 – not reached); $p < 0.01$]. **B**. PFS [median (95% confidence interval)] in patients with TIM3-positive tumor cells is significantly longer than in those with TIM3-negative tumor cells [18.9 months (6.7 – not reached) versus 1.1 months (0.5–17.5), $p < 0.01$].

Table 3
Expression of TIM3-related molecules in post-anti-PD-1 therapy samples.

Case	Regimen of IO therapy	BOR	Area of tumor tissues	IHC findings		
				TIM3 expression	HMGB1 localization	Accumulation of CD163 macrophages
Case 1	Nivo	CR	Necrotic area	+	Ex	+
Case 2	Nivo	SD	Necrotic area	+	Ex	+
			Viable area	+	N	–
Case 3	Nivo	PD	Viable area	–	N	–
Case 4	Nivo+Ipi	PR	Necrotic area	+	Ex	+
			Viable area	+	N	–
Case 5	Nivo+Ipi	PR	Necrotic area	+	Ex	+
			Viable area	+	N	–

IO; immune-oncology, IHC; immunohistochemistry, BOR; best overall response.
Nivo; Nivo monotherapy, Nivo+Ipi; Nivo+Ipi therapy, CR; complete response, PR; partial response, SD; stable disease, PD; progressive disease, Ex; extra-nuclear region, N; nucleus.

correlates with poor prognosis in lung cancer and breast cancer [31,32]. Hirsch et al. [33] reported variation of PD-L1 expression on tumor cells in lung cancer depending on the type of PD-L1 assay. The discrepancy of our finding with previous reports may be due to histological heterogeneity, higher proportion of poor risk patients in this study, and also the type of antibody used.

In the present study, more than one-half of pretreatment samples were obtained by CT-guided biopsy. Our study population contained a larger proportion of patients classified as poor risk according to IMDC compared to the populations in clinical trials of anti-PD-1 therapy (44% in our study versus 23% in nivolumab group of Checkmate 025 trial versus 21% in nivolumab plus ipilimumab group of Checkmate 214 trial), and also included five patients with KPS below 70%, which is an exclusion criteria in clinical trials [2,3]. Current RCC therapeutic guideline recommends avoiding cytoreductive nephrectomy in metastatic RCC patients with poor risk and low performance status because of limited survival benefit and high perioperative risk [34]. Higher proportion of patients with poor risk and poor performance status was the reason why we obtained pretreatment samples by CT-guided biopsy. Accurate assessment of tumor microenvironment seems to be difficult using a biopsy specimen because intra-tumoral heterogeneity exists in RCC [35,36]. Zahoor et al. [37] compared TILs between matched biopsy and nephrectomy samples from patients. They demonstrated a positive correlation between the frequencies of TILs in biopsy and nephrectomy samples, and concluded that biopsy material can be used for IHC analysis to provide insights into the tumor microenvironment. Based on these results, we performed IHC analyses using both biopsy and surgical specimens before initiation of systemic therapy. To decrease selective bias due to tumor heterogeneity, we acquired multiple images from both the central and peripheral regions of the tumor specimens and averaged the quantitative data of all images.

The function of TIM3 in tumor cells remains uncertain at present. TIM3 has been shown to be expressed on T cells, macrophages and dendric cells, and play a role as negative regulator of cytotoxic T cell viability [13,38,39]. Recently, TIM-3 expression on tumor cells has also been found in melanoma, liver cancer, lung cancer, and prostate cancer [40–42]. An analysis using the TCGA database indicated that the TIM3 gene amplification rate in RCC is higher compared to other types of cancer. The TIM3 gene is located on chromosome 5q which has been reported to be frequently amplified in RCC [43]. Recent study has revealed that 3p loss generates concurrent 5q gain as a result of chromothripsis event in the process of renal carcinogenesis [44]. Although the intracellular signaling mechanism of TIM3 has not been elucidated [28], we speculate that chromosomal amplification is one of the mechanisms of overexpression of TIM3 in RCC.

In RCC, the prognostic relevance of TIM3 expression on tumor cells remains controversial. Komohara, et al. [19] demonstrated high TIM3 expression in patients with relatively short PFS. On the contrary, Zhang,

et al. [45] reported TIM3 expression as a favorable prognostic factor for PFS and OS. They also showed higher detection rate of TIM3 in primary sites than in metastatic sites and homogeneous expression of TIM3 across different metastatic sites [45]. Therefore, we explored the significance of the presence of TIM3 expression in primary sites as a potential prognostic marker of anti-PD-1 therapy. We previously reported one case of CR to Nivo monotherapy for metastatic RCC, and that case showed expansion of necrosis in the tumor [30]. TIM3 plays a crucial role in mediating phagocytosis, which is one of the mechanisms of necrosis due to clearance of apoptotic cells by phagocytes such as macrophages [46,47]. Among the ligands of TIM3, HMGB1 is a necrosis-related ligand [28]. Therefore, we used post-treatment samples from 5 cases to analyze the relation between anti-PD-1 therapy-induced necrosis and TIM3, and analyzed macrophage infiltration and expression of HMGB1 which is released from nucleus during phagocytosis [29]. TIM3 expression was detected on cell membrane in all cases except the autopsy case with PD. Release of HMGB1 from nucleus was detected only in the necrotic tumor area after anti-PD-1 therapy. CD163 macrophage accumulated around the necrotic area in the responders. Based on these results, we speculate that TIM3 alone may not be sufficient to predict efficacy, but assessment of both TIM3 and HMGB1 may better predict tumor necrosis response to anti-PD-1 therapy. Extranuclear HMGB1 release can be monitored directly or indirectly using commercially available ELISA kits [48]. In the future, we plan to evaluate TIM3 expression on tumor cells before starting anti-PD-1 therapy and then measure plasma HMGB1 during anti-PD-1 therapy.

Our study had several limitations. It was a retrospective study with a small number of cases and potential selection bias. The sample does not provide sufficient power to perform quantitative multi-IF analyses for each regimen of anti-PD-1 therapy. Moreover, comparison of pre-treatment and post-treatment samples was not possible, since post-treatment samples were available from only 5 cases because many patients enrolled had poor risk or low performance status. Hence, the interaction between TIM3 and anti-PD-1 therapy was not elucidated. Our multi-immunofluorescence staining panel containing TIM3 (panel 1) did not include antibodies specific to immune cells other than T cells. Therefore, we did not evaluate total TIM3-related tumor immunity. In the future, we aim to establish multi-immunofluorescence staining panel that includes antibodies specific to other types of immune cells and to TIM3. We are also planning to use Autostainer to analyze a large number of pre-treatment and post-treatment samples to validate the usefulness of TIM3 expression as a biomarker of response to anti-PD-1 therapy. Furthermore, we need to perform analyses of mRNA expression and copy number alteration of TIM3 to evaluate the mechanism of overexpression of TIM3 protein.

In conclusion, our study found a clinical association between TIM3 expression on tumor cells and efficacy of anti-PD-1 therapy. In addition, analyses of samples obtained after starting anti-PD-1 therapy indicated that release of HMGB1 from the nucleus may trigger anti-PD-1 therapy-induced necrosis in patients showing TIM3 expression on tumor cells. Further studies are warranted to verify whether TIM3 expression on tumor cells before systemic therapy predicts the efficacy of anti-PD-1 therapy for RCC.

Declaration of Competing Interest

All authors have no potential conflicts of interest to disclose

CRediT authorship contribution statement

Renpei Kato: Conceptualization, Methodology, Formal analysis, Investigation, Resources, Data curation, Writing - original draft, Visualization, Project administration. **Noriaki Jinnouchi:** Formal analysis, Investigation, Writing - review & editing, Visualization. **Takashi Tuyukubo:** Validation, Writing - review & editing. **Daiki Ikarashi:** Validation, Writing - review & editing. **Tomohiko Matsuura:** Resources, Writing - review & editing. **Shigekatsu Maekawa:** Resources, Writing - review & editing. **Yoichiro Kato:** Resources, Data curation, Writing - review & editing, Supervision. **Mitsugu Kanehira:** Resources, Writing - review & editing, Supervision. **Ryo Takata:** Resources, Writing - review & editing, Supervision. **Kazuyuki Ishida:** Validation, Writing - review & editing. **Wataru Obara:** Conceptualization, Resources, Writing - original draft, Project administration.

Acknowledgments

The authors thank Reiko Shinagawa for technical assistance.

Funding

No specific funding was received.

Supplementary materials

Supplementary material associated with this article can be found, in the online version, at doi:10.1016/j.tranon.2020.100918.

References

[1] R.L. Siegel, K.D. Miller, A Jemal, Cancer statistics, 2020, CA Cancer J. Clin. 70 (1) (2020) 7–30.
[2] R.J. Motzer, B. Escudier, D.F. McDermott, S. George, H.J. Hammers, S. Srinivas, et al., Nivolumab versus everolimus in advanced renal-cell carcinoma, N. Engl. J. Med. 373 (19) (2015) 1803–1813.
[3] R.J. Motzer, N.M. Tannir, D.F. McDermott, O. Aren Frontera, B. Melichar, T.K. Choueiri, et al., Nivolumab plus ipilimumab versus sunitinib in advanced renal-cell carcinoma, N. Engl. J. Med. 378 (14) (2018) 1277–1290.
[4] B.I. Rini, E.R. Plimack, V. Stus, R. Gafanov, R. Hawkins, D. Nosov, et al., Pembrolizumab plus axitinib versus sunitinib for advanced renal-cell carcinoma, N. Engl. J. Med. 380 (12) (2019) 1116–1127.
[5] R.J. Motzer, K. Penkov, J. Haanen, B. Rini, L. Albiges, M.T. Campbell, et al., Avelumab plus axitinib versus sunitinib for advanced renal-cell carcinoma, N. Engl. J. Med. 380 (12) (2019) 1103–1115.
[6] J.M. Taube, A. Klein, J.R. Brahmer, H. Xu, X. Pan, J.H. Kim, et al., Association of PD-1, PD-1 ligands, and other features of the tumor immune microenvironment with response to anti-PD-1 therapy, Clin. Cancer Res.: Off. J. Am. Assoc. Cancer Res. 20 (19) (2014) 5064–5074.
[7] J. Konishi, K. Yamazaki, M. Azuma, I. Kinoshita, H. Dosaka-Akita, M Nishimura, B7-H1 expression on non-small cell lung cancer cells and its relationship with tumor-infiltrating lymphocytes and their PD-1 expression, Clin. Cancer Res.: Off. J. Am. Assoc. Cancer Res. 10 (15) (2004) 5094–5100.
[8] R.H. Thompson, M.D. Gillett, J.C. Cheville, C.M. Lohse, H. Dong, W.S. Webster, et al., Costimulatory B7-H1 in renal cell carcinoma patients: indicator of tumor aggressiveness and potential therapeutic target, Proc. Natl. Acad. Sci. USA 101 (49) (2004) 17174–17179.
[9] D.S. Shin, A. Ribas, The evolution of checkpoint blockade as a cancer therapy: what's here, what's next? Curr. Opin. Immunol. 33 (2015) 23–35.
[10] R.W. Griffiths, E. Elkord, D.E. Gilham, V. Ramani, N. Clarke, P.L. Stern, et al., Frequency of regulatory T cells in renal cell carcinoma patients and investigation of correlation with survival, Cancer Immunol. Immunother. 56 (11) (2007) 1743–1753.
[11] S.A. Siddiqui, X. Frigola, S. Bonne-Annee, M. Mercader, S.M. Kuntz, A.E. Krambeck, et al., Tumor-infiltrating Foxp3(-)CD4(+)CD25(+) T cells predict poor survival in renal cell carcinoma, Clin. Cancer Res. 13 (7) (2007) 2075–2081.
[12] K. Hotta, M. Sho, K. Fujimoto, K. Shimada, I. Yamato, S. Anai, et al., Prognostic significance of CD45RO+ memory T cells in renal cell carcinoma, Br. J. Cancer 105 (8) (2011) 1191–1196.
[13] C. Granier, C. Dariane, P. Combe, V. Verkarre, S. Urien, C. Badoual, et al., Tim-3 expression on tumor-infiltrating PD-1(+)CD8(+) T cells correlates with poor clinical outcome in renal cell carcinoma, Cancer Res. 77 (5) (2017) 1075–1082.
[14] Y. Komohara, H. Hasita, K. Ohnishi, Y. Fujiwara, S. Suzu, M. Eto, et al., Macrophage infiltration and its prognostic relevance in clear cell renal cell carcinoma, Cancer Sci. 102 (7) (2011) 1424–1431.
[15] Y. Huang, S. Goel, D.G. Duda, D. Fukumura, R.K Jain, Vascular normalization as an emerging strategy to enhance cancer immunotherapy, Cancer Res. 73 (10) (2013) 2943–2948.
[16] E. Yildiz, G. Gokce, H. Kilicarslan, S. Ayan, O.F. Goze, E.Y Gultekin, Prognostic value of the expression of Ki-67, CD44 and vascular endothelial growth factor, and microvessel invasion, in renal cell carcinoma, BJU Int. 93 (7) (2004) 1087–1093.
[17] T.K. Choueiri, D.J. Figueroa, A.P. Fay, S. Signoretti, Y. Liu, R. Gagnon, et al., Correlation of PD-L1 tumor expression and treatment outcomes in patients with renal cell carcinoma receiving sunitinib or pazopanib: results from COMPARZ, a randomized controlled trial, Clin. Cancer Res.: Off. J. Am. Assoc. Cancer Res. 21 (5) (2015) 1071–1077.
[18] J.H. Yearley, C. Gibson, N. Yu, C. Moon, E. Murphy, J. Juco, et al., PD-L2 expression in human tumors: relevance to anti-PD-1 therapy in cancer, Clin. Cancer Res.: Off. J. Am. Assoc. Cancer Res. 23 (12) (2017) 3158–3167.

[19] Y. Komohara, T. Morita, D.A. Annan, H. Horlad, K. Ohnishi, S. Yamada, et al., The coordinated actions of TIM-3 on cancer and myeloid cells in the regulation of tumorigenicity and clinical prognosis in clear cell renal cell carcinomas, Cancer Immunol. Res. 3 (9) (2015) 999–1007.
[20] E.R. Parra, N. Uraoka, M. Jiang, P. Cook, D. Gibbons, M.-.A. Forget, et al., Validation of multiplex immunofluorescence panels using multispectral microscopy for immune-profiling of formalin-fixed and paraffin-embedded human tumor tissues, Sci. Rep. 7 (1) (2017) 13380.
[21] W. Hugo, J.M. Zaretsky, L. Sun, C. Song, B.H. Moreno, S. Hu-Lieskovan, et al., Genomic and transcriptomic features of response to anti-PD-1 therapy in metastatic melanoma, Cell 165 (1) (2016) 35–44.
[22] M. Merkenschlager, L. Terry, R. Edwards, P.C.L Beverley, Limiting dilution analysis of proliferative responses in human lymphocyte populations defined by the monoclonal antibody UCHL1: implications for differential CD45 expression in T cell memory formation, Eur. J. Immunol. 18 (11) (1988) 1653–1662.
[23] D.M. Pardoll, The blockade of immune checkpoints in cancer immunotherapy, Nat. Rev. Cancer 12 (4) (2012) 252–264.
[24] E.C. Stack, C. Wang, K.A. Roman, C.C Hoyt, Multiplexed immunohistochemistry, imaging, and quantitation: a review, with an assessment of Tyramide signal amplification, multispectral imaging and multiplex analysis, Methods 70 (1) (2014) 46–58.
[25] S. Chiba, M. Baghdadi, H. Akiba, H. Yoshiyama, I. Kinoshita, H. Dosaka-Akita, et al., Tumor-infiltrating DCs suppress nucleic acid-mediated innate immune responses through interactions between the receptor TIM-3 and the alarmin HMGB1, Nat. Immunol. 13 (9) (2012) 832–842.
[26] E. Cerami, J. Gao, U. Dogrusoz, B.E. Gross, S.O. Sumer, B.A. Aksoy, et al., The cBio cancer genomics portal: an open platform for exploring multidimensional cancer genomics data, Cancer Discov. 2 (5) (2012) 401–404.
[27] J. Gao, B.A. Aksoy, U. Dogrusoz, G. Dresdner, B. Gross, S.O. Sumer, et al., Integrative analysis of complex cancer genomics and clinical profiles using the cBioPortal, Sci. Signal. 6 (269) (2013) pl1.
[28] Y. Wolf, A.C. Anderson, V.K Kuchroo, TIM3 comes of age as an inhibitory receptor, Nat. Rev. Immunol. 20 (3) (2020) 173–185.
[29] M.T. Lotze, K.J Tracey, High-mobility group box 1 protein (HMGB1): nuclear weapon in the immune arsenal, Nat. Rev. Immunol. 5 (4) (2005) 331–342.
[30] D. Ikarashi, Y. Kato, H. Katagiri, T. Takahara, N. Uesugi, E. Shiomi, et al., Case of complete response to neoadjuvant therapy using nivolumab in a patient with metastatic renal cell carcinoma, Int. J. Urol.: Off. J. Jpn. Urol. Assoc. 25 (6) (2018) 630–632.
[31] K. Takada, T. Okamoto, F. Shoji, M. Shimokawa, T. Akamine, S. Takamori, et al., Clinical significance of PD-L1 protein expression in surgically resected primary lung adenocarcinoma, J. Thorac. Oncol. 11 (11) (2016) 1879–1890.
[32] M.H. Zhang, H.B. Sun, S. Zhao, Y. Wang, H.H. Pu, Y. Wang, et al., Expression of PD-L1 and prognosis in breast cancer: a meta-analysis, Oncotarget 8 (19) (2017) 31347–31354.
[33] F.R. Hirsch, A. McElhinny, D. Stanforth, J. Ranger-Moore, M. Jansson, K. Kulangara, et al., PD-L1 Immunohistochemistry assays for lung cancer: results from phase 1 of the blueprint PD-L1 IHC assay comparison project, J. Thorac. Oncol. 12 (2) (2017) 208–222.
[34] A. Bex, L. Albiges, B. Ljungberg, K. Bensalah, S. Dabestani, R.H. Giles, et al., Updated European Association of Urology Guidelines for cytoreductive nephrectomy in patients with synchronous metastatic clear-cell renal cell carcinoma, Eur. Urol. 74 (6) (2018) 805–809.
[35] M. Gerlinger, A.J. Rowan, S. Horswell, M. Math, J. Larkin, D. Endesfelder, et al., Intratumor heterogeneity and branched evolution revealed by multiregion sequencing, N. Engl. J. Med. 366 (10) (2012) 883–892.
[36] S. Turajlic, H. Xu, K. Litchfield, A. Rowan, S. Horswell, T. Chambers, et al., Deterministic evolutionary trajectories influence primary tumor Growth: tRACERx renal, Cell 173 (3) (2018) 595–610.e11.
[37] H. Zahoor, P.G. Pavicic Jr., C. Przybycin, J. Ko, L. Stephens, T. Radivoyevitch, et al., Evaluation of T cell infiltration in matched biopsy and nephrectomy samples in renal cell carcinoma, Medicine 97 (37) (2018) e12344.
[38] J. Fourcade, Z. Sun, M. Benallaoua, P. Guillaume, I.F. Luescher, C. Sander, et al., Upregulation of Tim-3 and PD-1 expression is associated with tumor antigen-specific CD8+ T cell dysfunction in melanoma patients, J. Exp. Med. 207 (10) (2010) 2175–2186.
[39] K. Sakuishi, L. Apetoh, J.M. Sullivan, B.R. Blazar, V.K. Kuchroo, A.C Anderson, Targeting Tim-3 and PD-1 pathways to reverse T cell exhaustion and restore anti-tumor immunity, J. Exp. Med. 207 (10) (2010) 2187–2194.
[40] Z. Wiener, B. Kohalmi, P. Pocza, J. Jeager, G. Tolgyesi, S. Toth, et al., TIM-3 is expressed in melanoma cells and is upregulated in TGF-beta stimulated mast cells, J. Investig. Dermatol. 127 (4) (2007) 906–914.
[41] H. Li, K. Wu, K. Tao, L. Chen, Q. Zheng, X. Lu, et al., Tim-3/galectin-9 signaling pathway mediates T-cell dysfunction and predicts poor prognosis in patients with hepatitis B virus-associated hepatocellular carcinoma, Hepatology 56 (4) (2012) 1342–1351.
[42] X. Zhuang, X. Zhang, X. Xia, C. Zhang, X. Liang, L. Gao, et al., Ectopic expression of TIM-3 in lung cancers: a potential independent prognostic factor for patients with NSCLC, Am. J. Clin. Pathol. 137 (6) (2012) 978–985.
[43] Y. Sato, T. Yoshizato, Y. Shiraishi, S. Maekawa, Y. Okuno, T. Kamura, et al., Integrated molecular analysis of clear-cell renal cell carcinoma, Nat. Genet. 45 (8) (2013) 860–867.
[44] T.J. Mitchell, S. Turajlic, A. Rowan, D. Nicol, J.H.R. Farmery, T. O'Brien, et al., Timing the landmark events in the evolution of clear cell renal cell cancer: tRACERx renal, Cell 173 (3) (2018) 611-23.e17.
[45] X. Zhang, X. Yin, H. Zhang, G. Sun, Y. Yang, J. Chen, et al., Differential expression of TIM-3 between primary and metastatic sites in renal cell carcinoma, BMC Cancer 19 (1) (2019) 49.
[46] M. Nakayama, H. Akiba, K. Takeda, Y. Kojima, M. Hashiguchi, M. Azuma, et al., Tim-3 mediates phagocytosis of apoptotic cells and cross-presentation, Blood 113 (16) (2009) 3821–3830.
[47] I.K. Poon, C.D. Lucas, A.G. Rossi, K.S Ravichandran, Apoptotic cell clearance: basic biology and therapeutic potential, Nat. Rev. Immunol. 14 (3) (2014) 166–180.
[48] O. Kepp, L. Senovilla, I. Vitale, E. Vacchelli, S. Adjemian, P. Agostinis, et al., Consensus guidelines for the detection of immunogenic cell death, Oncoimmunology 3 (9) (2014) 19.